Variational solutions of simple quantum systems subject to variable boundary conditions. II. Shallow donor impurities near semiconductor interfaces: Si, Ge

Donald B. MacMillen and Uzi Landman
School of Physics, Georgia Institute of Technology, Atlanta, Georgia 30332
(Received 1 November 1983)

Variational solutions to the effective-mass equations describing hydrogenic donor impurities located near semiconductor-vacuum and semiconductor-insulator interfaces are presented and discussed. Results for the ground and excited eigenstate, binding energy, and spectra as a function of the location of the impurity from the semiconductor-vacuum interface are presented for Si(001) and Ge(111) surfaces. The electronic binding energy of a hydrogenic donor impurity as a function of its distance from the interface both into the insulator or into the semiconductor is studied in detail for the Si-SiO_2 case. The effect of an external electric field on the impurity binding energy is investigated and the results are compared with other recent theoretical calculations and experimental data.

INTRODUCTION

The electrical and optical properties of bulk semiconductors and of semiconductor interfaces [either with vacuum of in metal-oxide-semiconductor (MOS) devices] are strongly affected by impurities.[1] In the case of a bulk semiconductor characterized by a dielectric constant ϵ and isotropic effective mass m^* the bound states associated with singly charged attractive Coulomb center impurities embedded in the semiconductor have (for a parabolic band) a hydrogenic spectrum, $E_n=-m^*e^2/2\epsilon^2\hbar^2n^2$, $n=1,2,\ldots$, with respect to the adjacent band edge. It was first pointed out by Levine[2] that when the impurity is placed at the semiconductor surface, the spectrum is modified. As argued by Levine, since the height of the surface barrier can be several electron volts [and in the case of Si-SiO_2, about 3 eV (Ref. 3)] and the binding energies of shallow donor impurities are of the order of millielectron volts, the surface can be modeled as an infinite potential barrier requiring that the electron wave function vanish at the boundary (the effect of the infinite-discontinuity approximation has been shown to be negligible[4]). In the context of the effective-mass approximation,[5–7] neglecting the image potential and band bending and assuming a spherical band, one obtains again, for an impurity located exactly at the surface, a hydrogenic energy-level spectrum subject to the selection rule that only states with $|l-m|$ being odd are allowed (i.e., s states are excluded).

Since that time there have been several investigations of the energies and properties of these states.[8–13] Bell[8] *et al.* used the selection rules of Levine and the bulk energies of silicon and germanium to calculate transition energies. Petukhov[9] *et al.* included image charges in the effective-mass Hamiltonian and performed a perturbation calculation on that system. Karpushin[10] extended that perturbative treatment with the inclusion of linear band bending near the surface. In a later article, Karpushin[11] used a variational method to calculate the binding energies of donors on silicon and germanium surfaces. It is important to note that all of these authors constrained the impurity to lie exactly on the surface.

Realistically, the impurity will be distributed in the near-interface region, rather than being localized at the interface. The first computation which considers such a situation is that of Godwin and Teft,[14] who employed a simple form of the trial wave functions for the ground and excited states in a variational calculation. A more complete basis set, including the effect of an external electric field (see Sec. II), has been employed by Lipari.[15]

Armed with the variational method which we have described in detail in a preceding paper[16] in this series (which will be referred to as paper I), we study in this paper[17] the spectra of shallow donor impurities near semiconductor interfaces (vacuum and MOS interfaces, including the effect of electric fields) within the context of the effective-mass approximation.

In Sec. I the case of a donor impurity near a semiconductor-vacuum interface is considered. Results are given for Si(001) and Ge(111) surfaces. In Sec. II a donor impurity near a semiconductor-to-insulator interface is investigated. The impurity is embedded in the semiconductor or in the insulator. Results are given for Si-SiO_2 as a function of the location of the impurity and under the influence of an external electric field. Comparison to previous theories[13,15] and experimental data is given.

I. SHALLOW DONOR IMPURITY NEAR A SEMICONDUCTOR SURFACE

We first consider a donor impurity embedded in the semiconductor near, but not necessarily at, the semiconductor-vacuum interface. In constructing the model Hamiltonian for this system several simplifying assumptions shall be made. First, because of the multiple minima of the conduction band in $\vec{k}$ space, the crystallographic orientation of the surface becomes important. When considering the (001) plane of silicon or the (111) plane of germanium there exists[3] two kinds of constant-energy ellipsoids, those with their major axis parallel to the surface and those with their major axis perpendicular to it. One of the results of Karpushin[11] is that the ellipsoids with

their major axes perpendicular to the surface give rise to a series of states which lie lower in energy than those with their major axis parallel to the surface. Consequently, only these types of ellipsoids will be considered, because this allows a simplification in the requirements of the boundary condition $\psi=0$ on the surface plane. In addition, we shall assume that there is no change in the band structure near the surface, such as the formation of a space-charge layer, so that there is no band bending near the surface. Finally, we shall be working in the one-valley effective-mass approximation.[18]

The preceding considerations lead to an effective-mass equation given by

$$\left[\frac{-\hbar^2}{2m_t^*}\left[\frac{\partial^2}{\partial x^2}+\frac{\partial^2}{\partial y^2}\right]-\frac{\hbar^2}{2m_l^*}\frac{\partial^2}{\partial z^2}-\frac{e^2}{\epsilon_1 r}+\frac{\epsilon_2-\epsilon_1}{\epsilon_1(\epsilon_1+\epsilon_2)}\frac{e^2}{(r^2+4R^2-4rR\cos\theta)^{1/2}}-\frac{(\epsilon_2-\epsilon_1)e^2}{4\epsilon_1(\epsilon_1+\epsilon_2)(R-r\cos\theta)}\right]F(\vec{r})=EF(\vec{r})\ . \quad (1.1)$$

This equation must be solved subject to the boundary condition

$$F(\vec{r})=0 \ \text{ when } r\cos\theta=R\ . \quad (1.2)$$

The impurity is located at a distance R from the planar interface (see Fig. 1). Note that Eq. (1.1) follows from the choice of the (001) surface for silicon or the (111) surface for germanium. In Eq. (1.1), m_t^* and m_l^* are the transverse and longitudinal effective masses, and ϵ_1 denotes the static dielectric constant of the region containing the impurity. The static dielectric constant of region B (see Fig. 1) is denoted by ϵ_2. This leaves open the option of solving for a semiconductor/insulator interface or a semiconductor/ vacuum interface. The last two terms on the right-hand side of Eq. (1.1) are the electron-image proton and the electron-image electron terms, respectively.

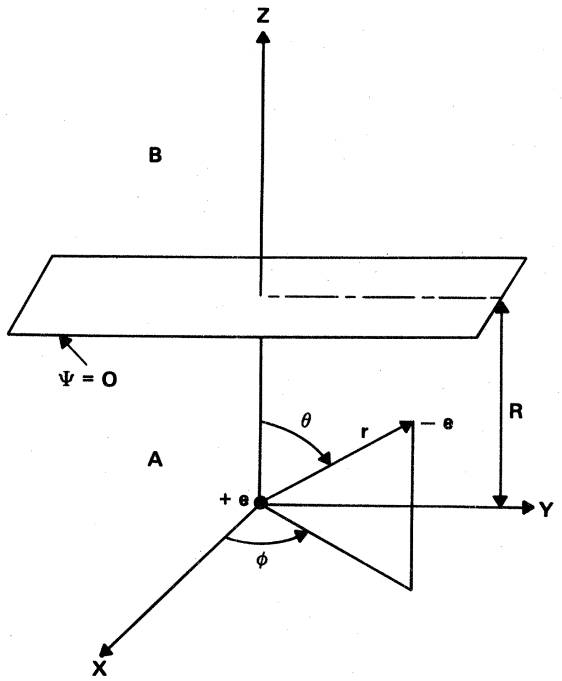

FIG. 1. Coordinate system of Eq. (1.1) centered at the hydrogenic impurity, and the boundary surface at $z=R-r\cos\theta$.

In the following we shall be concerned with solving a scaled version of Eq. (1.1). All distances, including R, the distance of the impurity from the surface plane, are scaled to units of effective Bohr radii given by

$$a_0^*=\frac{\hbar^2\epsilon_1}{m_t^* e^2}=0.529\left[\frac{\epsilon_1 m}{m_t^*}\right]\text{ Å}\ , \quad (1.3)$$

and the energy is in units of effective rydbergs,

$$\text{Ry}^*=\frac{m_t^* e^4}{2\hbar^2\epsilon_1^2}=13.6\left[\frac{m_t^*}{m}\frac{1}{\epsilon_1^2}\right]\text{ eV}\ . \quad (1.4)$$

The scaled version of Eq. (1.1) is then given by

$$\left[-\left[\frac{\partial^2}{\partial x^2}+\frac{\partial^2}{\partial y^2}+\gamma\frac{\partial^2}{\partial z^2}\right]-\frac{2}{r}+\frac{2Q}{(r+4R^2-4rR\cos\theta)^{1/2}}-\frac{Q}{(2R-r\cos\theta)}\right]F(\vec{r})=EF(\vec{r})\ , \quad (1.5)$$

where Q is given by

$$Q=(\epsilon_2-\epsilon_1)/(\epsilon_2+\epsilon_1)\ , \quad (1.6)$$

and γ is the effective-mass ratio defined as $\gamma=m_t^*/m_l^*$. We note in passing that the effective-mass equation has been scaled to the bulk semiconductor parameters rather than the surface units defined by Stern and Howard.[3] This scaling has been chosen for easier comparison to the bulk limit (R becomes large), and also because this choice yields the factor $(\epsilon_2-\epsilon_1)/(\epsilon_1+\epsilon_2)$. This factor always lies between -1 and 1, whereas this is not the case for surface units. This feature is a practical one since large constants multiplying matrix elements are undesirable in the solution of the matrix equations.

In the solution of Eq. (1.5), subject to the boundary conditions of Eq. (1.2), a strategy that is a combination of a variational method described in Paper I (Ref. 16) with a method presented by Faulkner[19] is used. In our previous study[16] we solved for the spectrum of a hydrogen atom approaching a surface where the exchange repulsion interaction between the atomic electron and the substrate was modeled via the surface boundary condition [Eq. (1.2)]. Our present Hamiltonian [Eq. (1.1)] is equivalent to that used in our previous paper when $m_t^*=m_l^*$ (i.e., iso-

tropic effective mass). Therefore the Hamiltonian used in this study differs from that used by us before only in the z dependence, and thus all the symmetry properties discussed by us previously[16] are valid. In particular, for finite R, m remains a good quantum number, while n and l do not. However, due to the symmetry properties of Eq. (1.5), the behavior when $R\rightarrow\infty$ (i.e., bulk hydrogenic impurity embedded in the semiconductor medium) is different in our present case from that encountered in the previous study. The effective-mass Hamiltonian is invariant under operations of parity and rotation about the z axis. This means that for the bulk impurity, n and l are no longer good quantum numbers, while m is; however, states of even and odd l are not mixed. Therefore, the effect of the boundary condition in this situation is to mix states of differing parity.

Since m remains a good quantum number, the problem can be reduced to a separate variational solution of Eq. (1.5) for each value of m. Consequently, the trial function for states characterized by a given value of m can be written as

$$F_m(\vec{r})=G(z)\sum_{n=1}^{N}\sum_{l=0}^{n-1}A_{(n,l)}^{(m)}\chi_{n+m,l+m,m}(\vec{r}) , \quad (1.7a)$$

where the choice of $G(z)=R-r\cos\theta$ is made in order to satisfy the interface boundary condition [Eq. (1.2)]. The χ_{nlm}'s are chosen as

$$\chi_{nlm}(x,y,z)=(\alpha/\gamma)^{1/4}\phi_{nlm}(x,y,(\alpha/\gamma)^{1/2}z,\beta) , \quad (1.7b)$$

where γ is the effective-mass ratio and α is another nonlinear variational parameter. The basis functions $\phi_{nlm}(\vec{r},\beta)$ are given by

$$\phi_{nlm}(\vec{r},\beta)=\frac{(2\beta)^{3/2}}{\sqrt{2n}}\left[\frac{(N-l-1)!}{[(N+l)!]^3}\right]^{1/2}$$

$$\times(2\beta r)^l L_{n-l-1}^{2l+1}(2\beta r)e^{-\beta r}Y_l^m(\theta,\phi) . \quad (1.7c)$$

In Eq. (1.7c) the Y_l^m are the usual spherical harmonics, the L_p^k are the associated Laguerre polynomials, and r is taken to be in units of effective Bohr radii, a_0^*. The difference between the set of functions given by Eq. (1.7c) and the isolated hydrogen-atom eigenfunctions is the appearance of the combination βr, where β is an additional variational parameter independent of any quantum number, rather than the combination r/n which depends upon the particular state under consideration. The advantages of this choice are twofold. First, the isolated hydrogen-atom orbitals do not form a complete set without the inclusion of the continuum states.[20] Use of the set given by (1.7c) has been shown to include contributions from these states.[21] Second, the virial theorem is automatically satisfied for any quantum-mechanical system whose potential is a homogeneous function of the coordinates, if a scale factor is introduced into the approximate wave function and varied so as to give the lowest energy.[22] The parameter β is such a scale factor, and because its optimum value will be found, the properties of the states found with the approximate wave functions of Eq. (1.7a) will be better than those which do not contain such a scaling. The parameter α is a measure of the asymmetry induced in the wave function due to the asymmetric effective mass. The choice of the functions given by Eq. (1.7b) was inspired by the success of the Kohn-Luttinger[5,6] form for the ground-state trial wave function; upon setting $\beta=1/a$ and $\alpha=a^2/b^2$, $\chi_{1,0,0}(x,y,z)$ reduces to their trial function. This basis set differs from that used by Faulkner inasmuch as we use the combination βr rather than $\beta r/n$ in the radial function where n is the principal quantum number. Therefore, for the calculations presented here there are only two nonlinear variational parameter, whereas Faulkner must use a set of such parameters, the number of which depends upon the size of the basis set used in the expansion of the trial function. Of course, this means that we must calculate an overlap matrix, but as it has been shown this is not a great handicap.

The variational solution of Eq. (1.5) using Eqs. (1.7) leads to a matrix eigenvalue problem which, due to the azimuthal symmetry, can be partitioned according to the m value, thus reducing to a set of matrix equations for $m=0,1,2,\ldots$. Hence,

$$\underline{H}^{(m)}\vec{A}^{(m)}=E\underline{N}^{(m)}\vec{A}^{(m)} , \quad (1.8)$$

where $\underline{H}^{(m)}$ and $\underline{N}^{(m)}$ are the Hamiltonian and overlap matrices and $\vec{A}^{(m)}$ is the vector of expansion coefficients.

The Hamiltonian matrix elements are given by

$$H_{n'l',nl}^{(m)}=\int_T(\alpha/\gamma)^{1/2}(R-r\cos\theta)\phi_{n'l'm}^*(x,y,(\alpha/\gamma)^{1/2}z,\beta)$$

$$\times\left[-\left[\frac{\partial^2}{\partial x^2}+\frac{\partial^2}{\partial y^2}+\gamma\frac{\partial^2}{\partial z^2}\right]-\frac{2}{r}+\frac{2Q}{(r^2+4R^2-4rR\cos\theta)^{1/2}}+\frac{Q}{2(R-r\cos\theta)}\right]$$

$$\times(R-r\cos\theta)\phi_{nlm}(x,y,(\alpha/\gamma)^{1/2}z,\beta)dV , \quad (1.9)$$

which, upon making the substitution $(\alpha/\gamma)^{1/2}z'=z$, yields

$$H^{(m)}_{n'l',nl}=\int_T [R-(\gamma/\alpha)^{1/2}r\cos\theta]\phi^*_{n'l'm}(x,y,z,\beta)$$
$$\times\left[-\left[\frac{\partial^2}{\partial x^2}+\frac{\partial^2}{\partial y^2}+\gamma\frac{\partial^2}{\partial z^2}\right]+(1-\alpha)\frac{\partial^2}{\partial z^2}-\frac{2}{[x^2+y^2+(\gamma/\alpha)z^2]^{1/2}}\right.$$
$$+\frac{2Q}{[x^2+y^2+(\gamma/\alpha)z^2+4R^2-4(\gamma/\alpha)^{1/2}rR\cos\theta]^{1/2}}$$
$$\left.-\frac{Q}{2[R-(\gamma/\alpha)^{1/2}r\cos\theta]}\right]\{[R-(\gamma/\alpha)^{1/2}r\cos\theta]\phi_{nlm}(x,y,z,\beta)\}dV\ . \quad (1.10)$$

The overlap matrix elements are given by

$$N^{(m)}_{n'l',nl}=\int_T [R-(\gamma/\alpha)^{1/2}r\cos\theta]^2$$
$$\times\phi^*_{n'l'm}(\vec{r},\beta)\phi_{nlm}(\vec{r},\beta)dV\ . \quad (1.11)$$

The subscript T in Eqs. (1.9)—(1.11) indicates truncated regions of integration. In the calculation of the matrix elements, the integration over the azimuthal variable ϕ yields $2\pi\delta_{m'm}$.

The matrix equation whose elements are given by Eqs. (1.10) and (1.11) shall be solved numerically. The first step in this direction is the calculation of the quantities

$$-\nabla^2[R-(\gamma/\alpha)^{1/2}r\cos\theta]\phi_{nlm}(\vec{r},\beta) \quad (1.12)$$

and

$$(1-\alpha)\frac{d^2}{dz^2}\{[R-(\gamma/\alpha)^{1/2}r\cos\theta]\phi_{nlm}(\vec{r},\beta)\}\ . \quad (1.13)$$

The first of these expressions [Eq. (1.12)] has already been encountered by us before [see paper I, Eqs. (1.11) and (1.16)]. The second yields a somewhat complicated sum of terms involving the Legendre and Laguere functions of various orders and will not be repeated here. Most of these terms can be integrated in closed form. However, for the third and fourth terms in Eq. (1.10) this was not found to be the case. Consequently, these terms were numerically integrated as previously described.

The general method of the numerical solution of the matrix equations is the same as described in the previous paper.[16] However, there is now an additional parameter, namely α, which must be varied to yield an optimized energy. In practice, the energy is a relatively slowly varying function of α near the optimum values of these quantities, and this feature eases the problems associated with locating a minimum in the two-parameter space. The calculation proceeds as follows. Given a distance from the interface R, a value of m ($m=0,1,2,\ldots$) is chosen. The ith eigenvalue, $E_i^{(m)}(R)$ ($i=1,2,\ldots$), of the corresponding eigenvalue matrix equation is then optimized with regard to variations in the parameters α and β for a chosen number of basis functions $N(N+1)/2$ included in the trial function, Eq. (1.7a) (note that the optimum values of α and β depend upon which eigenvalue is being minimized). This procedure is then repeated for $N+1$ until convergence to a certain number of significant figures in the calculated eigenvalues is achieved. In our calculations we found that taking $N=7$ yields results accurate to four significant figures.

TABLE I. Values of physical constants.

	γ	ϵ	a_0^* (Å)	Ry* (meV)
Si	0.2079	11.4	31.7	19.9
Ge	0.051 34	15.36	99.7	4.7

Prior to discussing the results of this section, all of which are presented in effective units, the various physical constants of silicon and germanium that are relevant to this problem are presented in Table I. The effective masses and corresponding γ values of Si and Ge are taken from Refs. 23 and 24, respectively. The static dielectric constants of silicon and germanium are taken from Faulkner,[19] who determined the low-temperature values of these dielectric constants by requiring that the donor spectrum calculated in the effective-mass approximation have an optimum fit to the experimentally determined donor level spacing. By using these values, the effective units for silicon are given by

$$(a_0^*)_{\rm Si}=\frac{\hbar^2\epsilon_{\rm Si}}{(m_t^*)_{\rm Si}e^2}=31.7\ \text{Å}\ , \quad (1.14a)$$

$$\text{Ry}^*_{\rm Si}=\frac{(m_t^*)_{\rm Si}e^4}{2\hbar^2\epsilon^2_{\rm Si}}=1.99\times10^{-2}\ \text{eV}\ , \quad (1.14b)$$

while those for germanium are

$$(a_0^*)_{\rm Ge}=99.7\ \text{Å},\quad \text{Ry}^*_{\rm Ge}=4.70\times10^{-3}\ \text{eV}\ . \quad (1.15)$$

In addition to the introduction of an anisotropic effective mass, the major difference from the problem of the preceding paper is that the "hydrogen atom" is now imbedded in a dielectric media and is near an interface with a media possessing a lower dielectric constant. This means that the image charges posses the same sign (positive or negative) as the charges that induce them. This can be seen from the form of the dielectric quotient given by $(\epsilon_2-\epsilon_1)/(\epsilon_1+\epsilon_2)$. This results in a repulsive electron—image-electron interaction, while the electron—image-proton interaction now becomes attractive.

The results of the "perfectly imaging" plane show that, at least for the ground state, the absolute value of the expectation value of the electron—image-proton interaction is greater than the expectation value of the electron—image-electron interaction. Since the former of these quantities is negative, at a sufficiently large distance

TABLE II. Ground-state properties of a shallow donor near the surface of a symmetric ($\gamma=1$) silicon. All quantities are given in bulk units defined by Eqs. (1.3) and (1.4). E_0 denotes the ground-state energy, $\bar{T}$ the average kinetic energy, and $\bar{V}_1$, $\bar{V}_2$, and $\bar{V}_3$ are the average values of the three potential terms in Eq. (1.5), respectively.

R	E_0	$\bar{T}$	$\bar{V}_1$	$\bar{V}_2$	$\bar{V}_3$
0.2	−0.6064	0.6373	−0.8658	0.2380	−0.6159
0.4	−0.6507	0.7670	−1.0594	0.2586	−0.6169
0.6	−0.7221	0.9696	−1.3522	0.2841	−0.6237
0.8	−0.8098	1.1662	−1.6626	0.3001	−0.6135
1.0	−0.8945	1.2853	−1.8972	0.3000	−0.5825
1.2	−0.9640	1.3268	−2.0379	0.2882	−0.5410
1.4	−1.0158	1.3204	−2.1092	0.2708	−0.4978
1.6	−1.0521	1.2912	−2.1381	0.2519	−0.4571
1.8	−1.0767	1.2539	−2.1434	0.2332	−0.4204
2.0	−1.0925	1.2160	−2.1364	0.2157	−0.3878
3.0	−1.1086	1.0827	−2.0674	0.1498	−0.2736
4.0	−1.0944	1.0302	−2.0273	0.1111	−0.2084
5.0	−1.0794	1.0121	−2.0115	0.0875	−0.1674
6.0	−1.0676	1.0057	−2.0056	0.0720	−0.1397

from the surface, the ground-state electronic energy is expected to be lower than the $R=\infty$ limit when there is no image-charge contribution. As the impurity is moved closer to the surface, the change in the energy due to the exclusion of the electron from the half-space $r\cos\theta \geq R$ will begin to dominate and begin to raise (as a function of the impurity distance from the surface) the ground-state energy. Therefore, we expect to see the development of a minimum in the ground-state electronic energy.

The results presented in Tables II–IV show that this is precisely what takes place. Table II presents the ground-state energy of an impurity near a silicon surface for $\gamma=1.0$; that is, as if silicon possessed a spherical conduction band. The bulk limit in this case is given by the hydrogenic -1.0 Ry*. Tables III and IV give the ground-state properties of a donor impurity near the (001) silicon surface and the (111) germanium surface, respectively. The bulk values for these two systems, in effective rydbergs, are given by[19]

$$E_0^{\mathrm{Si}}(R\to\infty)=-1.568\ \mathrm{Ry}^*_{\mathrm{Si}}\,, \tag{1.16a}$$

$$E_0^{\mathrm{Ge}}(R\to\infty)=-2.087\ \mathrm{Ry}^*_{\mathrm{Ge}}\,. \tag{1.16b}$$

As a calculational check, the energies of these ground states were computed at a distance from the surface of $100a_0^*$, yielding

$$E_0^{\mathrm{Si}}(R=100(a_0^*)_{\mathrm{Si}})=-1.571\ \mathrm{Ry}^*_{\mathrm{Si}}\,, \tag{1.17a}$$

$$E_0^{\mathrm{Ge}}(R=100(a_0^*)_{\mathrm{Ge}})=-2.094\ \mathrm{Ry}^*_{\mathrm{Ge}}\,, \tag{1.17b}$$

which is in agreement with the bulk values to within 0.1%.

The ground-state energies of the "isotropic effective-mass" silicon and the real silicon systems are presented graphically in Fig. 2, while those for the germanium system are given in Fig. 3. There are basically three regions of different behavior depicted in these graphs. At large R the impurity levels are approaching their indicated bulk levels. Also, there now exist minima which occur at approximately $2.6a_0^*$, $1.0a_0^*$, and $0.5a_0^*$ for the "isotropic" silicon, real silicon, and germanium systems, respectively. Finally, when the impurity is close to the surface there is a steep rise in the electronic energy. The main difference in the behavior of the energy as a function of the impurity distance from the surface between these three systems lies in the location and the depth of the energy minimum. This difference is due to the changing value of γ, the effective-mass ratio, and can be explained in the following manner. In the bulk situation, the change in the wave function due to $\gamma<1.0$ in Eq. (1.5) allows for a *compression* of the wave function slightly in the z direction.[6] Since the surface is perpendicular to the z axis, this means that an impurity wave function for a specific value of the effective-mass ratio will experience a lesser perturbation than the wave function corresponding to a large value of

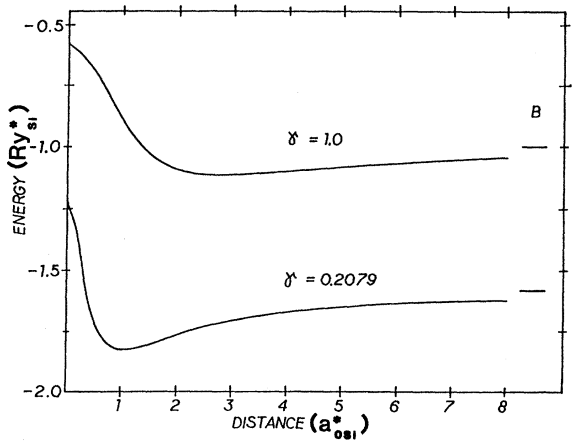

FIG. 2. Ground-state energy of a shallow donor impurity near the (001) surface of silicon. Also included are the results for an isotropic effective mass. The bulk values are given by the lines under the B. Units are those of effective rydbergs and effective Bohr radii as defined in text.

TABLE III. Ground-state properties of a shallow donor near the (001) surface of silicon. ($\gamma=0.2079$; entries and units are as in Table II.)

R	E	$\bar{T}$	$\bar{V}_1$	$\bar{V}_2$	$\bar{V}_3$
0.2	−1.3601	1.3555	−2.0850	0.6374	−1.2679
0.4	−1.5927	1.6827	−2.7632	0.6695	−1.1817
0.6	−1.7496	1.8436	−3.1709	0.6084	−1.0307
0.8	−1.8133	1.8267	−3.2815	0.5165	−0.8750
1.0	−1.8278	1.7695	−3.2845	0.4345	−0.7472
1.2	−1.8210	1.7255	−3.2681	0.3685	−0.6469
1.4	−1.8061	1.6701	−3.2350	0.3167	−0.5670
1.6	−1.7890	1.6466	−3.2085	0.2762	−0.5032
1.8	−1.7722	1.6243	−3.1891	0.2441	−0.4515
2.0	−1.7568	1.6094	−3.1755	0.2183	−0.4089
3.0	−1.7013	1.5796	−3.1469	0.1425	−0.2765
4.0	−1.6697	1.5723	−3.1396	0.1060	−0.2084
5.0	−1.6499	1.5698	−3.1372	0.0845	−0.1671
6.0	−1.6365	1.5688	−3.1361	0.0702	−0.1394

the effective-mass ratio. Consequently, the minimum in energy will occur at smaller *scaled* distances from the surface as the value of the effective-mass ratio is decreased. Note that this argument is true only for the *scaled* Hamiltonian, and that the minimum energy of a donor in germanium occurs at a *larger* distance than it does for a donor in silicon.

The excited-state energies for a donor impurity near the (001) surface of silicon and the (111) surface of germanium are presented in Figs. 4 and 5. The approach to the bulk values of the energy levels of the excited states takes place at a slower rate due to the larger "spatial" extent of these states. Note that because the states labeled (0,3) and (1,1) (the first label refers to the value of the m quantum number, while the second give its position in the spectrum of levels with the same m quantum number) possess different azimuthal quantum numbers, there is not, as it might appear, an avoided crossing between them.

Finally, we note that using the results for the ground-state electronic energy given in Tables II–IV, the impurity-surface "holding potentials," consisting of the change in the electronic energy from its bulk value and the interaction of the positive impurity with its image, can be calculated (similar to the physisorption holding potential calculated in Sec. II of Paper I). The results suggest a tendency of the impurities to be concentrated near the semiconductor surface (at distances of 20–50 Å from the interface).

II. SHALLOW DONOR IMPURITY NEAR THE Si/SiO_2 INTERFACE OF A MOS FIELD-EFFECT TRANSISTOR

The acronym MOSFET is derived from the combination metal-oxide-semiconductor field-effect transistor. The metal gate is used to apply an electric field perpendicular to the surface of the semiconductor, from which it is insulated by an oxide layer. An n-type inversion layer can be produced in a p-type semiconductor at the surface if the energy bands near the surface are sufficiently bent down so that the bottom of the conduction band lies near or below the Fermi level. Such a situation is referred to as an inversion layer, since the majority-carrier type in that region is the opposite of the bulk majority carrier. The

TABLE IV. Ground-state properties of a shallow donor near the (111) surface of germanium. ($\gamma=0.051\,34$; entries and units are as in Table II.)

R	E	$\bar{T}$	$\bar{V}_1$	$\bar{V}_2$	$\bar{V}_3$
0.2	−2.3013	2.2378	−3.7971	1.2923	−2.0343
0.4	−2.5389	2.4841	−4.4397	1.0238	−1.6071
0.6	−2.5485	2.4160	−4.4679	0.7463	−1.2428
0.8	−2.5035	2.2929	−4.3725	0.5673	−0.9912
1.0	−2.4538	2.2164	−4.3039	0.4523	−0.8185
1.2	−2.4104	2.1721	−4.2622	0.3747	−0.6951
1.4	−2.3743	2.1460	−4.2369	0.3195	−0.6030
1.6	−2.3447	2.1298	−4.2211	0.2785	−0.5320
1.8	−2.3203	2.1194	−4.2108	0.2469	−0.4757
2.0	−2.2998	2.1124	−4.2038	0.2216	−0.4300
3.0	−2.2343	2.0981	−4.1896	0.1470	−0.2898
4.0	−2.1980	2.0943	−4.1848	0.1100	−0.2183
5.0	−2.1785	2.0132	−4.1847	0.0879	−0.1749

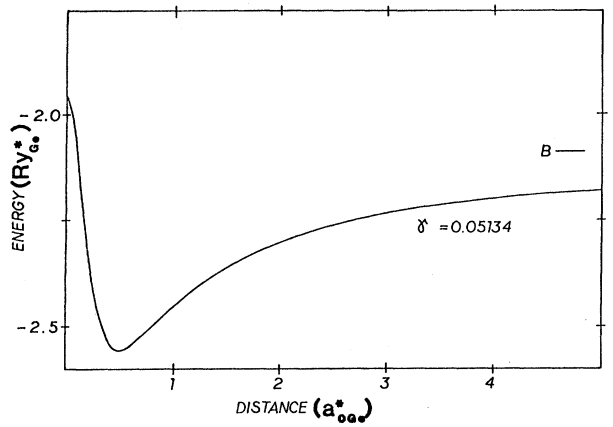

FIG. 3. Ground-state energy of a shallow donor impurity near the (111) surface of germanium. Effective Ge units are used.

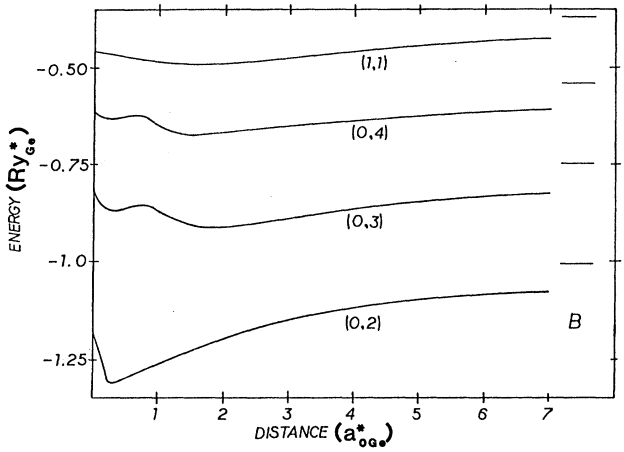

FIG. 5. Excited states of a shallow donor impurity near the (111) surface of germanium. Effective Ge units are used.

band bending required to produce an inversion layer can be produced from the field applied by the metal gate.

If the electric field is sufficiently strong, electrons in the conduction band can become quantized in the direction perpendicular to the surface, while remaining in a continuum for motion parallel to the surface. One of these quantized states is known as an electric subband, and to a good first approximation these subband energies can be modeled as the eigenvalues of a one-dimensional potential well.[3] When the gate voltage is sufficiently large, an essentially two-dimensional conductance can be observed between the electrodes marked source and drain.

Recently, Hartstein and Fowler[25,26,1] have observed an effect in the conductance, as a function of gate voltage, in a MOSFET that can be attributed to the formation of an impurity band. Briefly, the experiment consisted of drifting Na^+ ions close to the $Si\text{-}SiO_2$ interface and then measuring the conductance of the channel as a function of gate voltage. What is observed is the appearance of a peak in the conductance below the threshold for two-dimensional metallic conduction. By measuring the conductivity of the peak as a function of temperature, the binding energy of an electron to one of the impurities can be determined from the slope of a plot of the logarithm of the conductivity versus the inverse of the temperature. We note here that the impurity is generally thought to be located several angstroms away from the interface into the oxide layer, while the electron is in the semiconductor inversion layer.

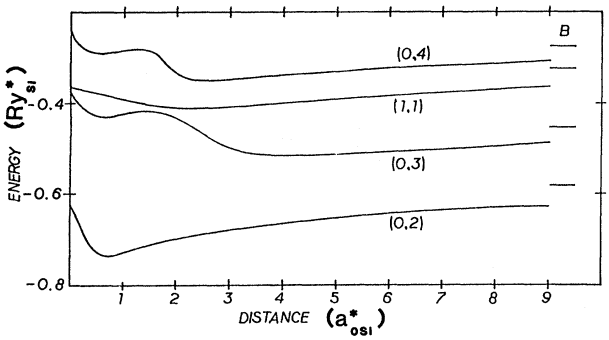

FIG. 4. Excited states of a shallow donor impurity near the (001) surface of silicon. Effective Si units are used.

As in the preceding section, only the (001) surface of silicon shall be considered. Now, however, the dielectric constant of region B (see Fig. 1) will be taken to be that of SiO_2, that is $\epsilon_2=3.8$. In the following, for the sake of comparison with other theoretical results, the dielectric constant of silcon shall be taken as $\epsilon_1=11.8$. Since the discontinuity in energy as an electron passes from the silicon to the silicon dioxide is about 3 eV,[3] the boundary condition $\psi=0$ at the interface shall again be applied.[3]

There are two modifications of the Hamiltonian of the preceding section which make it applicable to the present problem. First, the positively charged impurity is located in the oxide layer which changes the constant factor in its interaction with the electron, and connected with this, the image of the impurity is absent. Second, the change in the potential energy of the electron due to the presence of the electric field must be taken into account. The electric field can be a complicated function of the perpendicular distance to the interface; however, a reasonable first approximation is to employ a constant field.[3]

These considerations lead us to a Hamiltonian given by

$$H=\frac{-\hbar^2}{2m_t^*}\left[\frac{\partial^2}{\partial x^2}+\frac{\partial^2}{\partial y^2}\right]-\frac{\hbar^2}{2m_l^*}\frac{\partial^2}{\partial z^2}-\frac{2e^2}{(\epsilon_1+\epsilon_2)r}$$

$$-\frac{(\epsilon_2-\epsilon_1)e^2}{4\epsilon_1(\epsilon_1+\epsilon_2)(R-r\cos\theta)}+e\mathscr{E}(R-r\cos\theta)\,, \qquad (2.1)$$

where ϵ_1 and ϵ_2 are the dielectric constants of silicon and silicon dioxide, respectively, and $\mathscr{E}$ is the local electric field. As before, this Hamiltonian is scaled to bulk units yielding

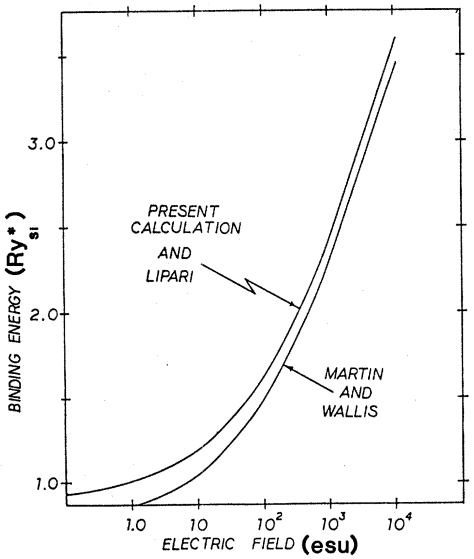

FIG. 6. Binding energy of an electron to a donor impurity located on the interface between the silicon and silicon dioxide as a function of electric field. Energy is in units of effective rydbergs, while the electric field is given in esu.

$$H=-\left[\frac{\partial^2}{\partial x^2}+\frac{\partial^2}{\partial y^2}\right]-\gamma\frac{\partial^2}{\partial z^2}-\frac{4\epsilon_1}{(\epsilon_1+\epsilon_2)r}$$
$$-\frac{\epsilon_2-\epsilon_1}{2(\epsilon_1+\epsilon_2)(R-r\cos\theta)}+2\epsilon_1^3\left[\frac{m}{m_t^*}\right]^2\mathscr{E}(R-r\cos\theta)\,. \tag{2.2}$$

The Schrödinger equation with the Hamiltonian given in Eq. (2.2) is to be solved subject to the condition that $\psi=0$ when $R=r\cos\theta$. All distances are in effective Bohr radii, and all energies are in effective rydbergs [Eq. (1.14)].

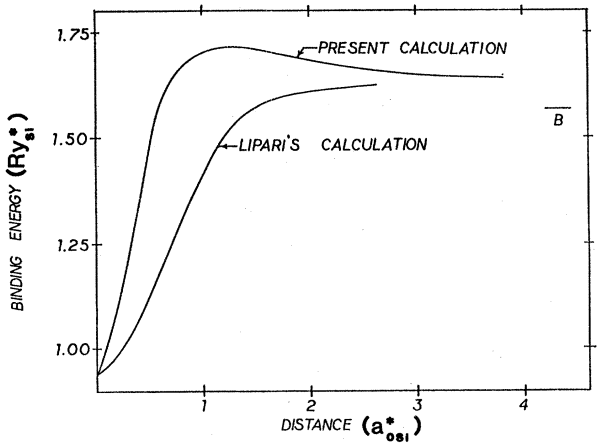

FIG. 7. Binding energy at zero field as a function of impurity distance into the silicon (semiconductor) layer.

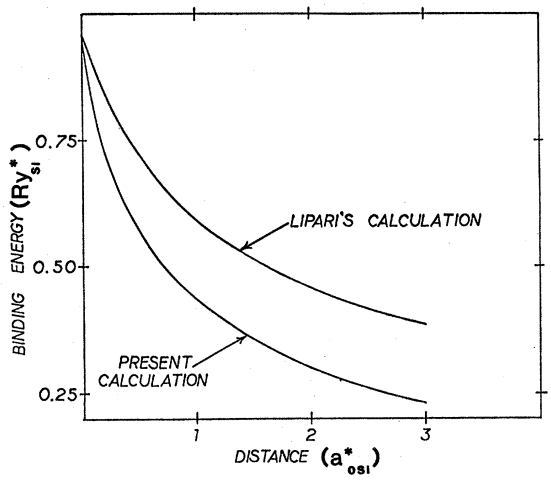

FIG. 8. Binding energy at zero field as a function of impurity distance into the silicon dioxide layer.

Once the matrix elements involving the field term have been included in the Hamiltonian matrix, the energy levels are obtained in the manner discussed previously.

The binding energy of the electron in the present case is not simply given as the absolute value of the ground state of Eq. (2.2). This is due to the fact that the electron is making a transition to the first electric subband and not to a bulklike conduction band. In the absence of the impurity potential, the Hamiltonian (2.2) becomes

$$H_0=-\gamma\frac{\partial^2}{\partial z^2}-\frac{\epsilon_2-\epsilon_1}{2(\epsilon_1+\epsilon_2)z}+K\mathscr{E}z\,. \tag{2.3}$$

In Eq. (2.3), $\mathscr{E}$ is to be given in electrostatic units, and therefore K has the value

$$K=1.166\times10^{-7}\epsilon_1^3\left[\frac{m}{m_t^*}\right]^2. \tag{2.4}$$

Of course, the electron in this system also experiences the potential jump upon entering the silicon dioxide and the boundary condition $\psi(0)=0$ must be applied.

If the repulsive image term of Eq. (2.3) was absent, the system would be the exactly solvable one of a triangular potential well where the eigenfunctions are given by the Airy functions. When the image term is present, a simple variational calculation yields very accurate values for the electric subband energy levels. A trial function of the form

$$\psi(z)=e^{-\alpha z/2}\sum_{n=0}^{N}A_n z^{n+1} \tag{2.5}$$

is chosen. Notice that this trial function satisfies the correct boundary conditions. As in the previous situations, the linear variational parameters A_n lead to a matrix equation whose eigenvalues are optimized by varying the parameter α. The binding energy of the electron is therefore given by

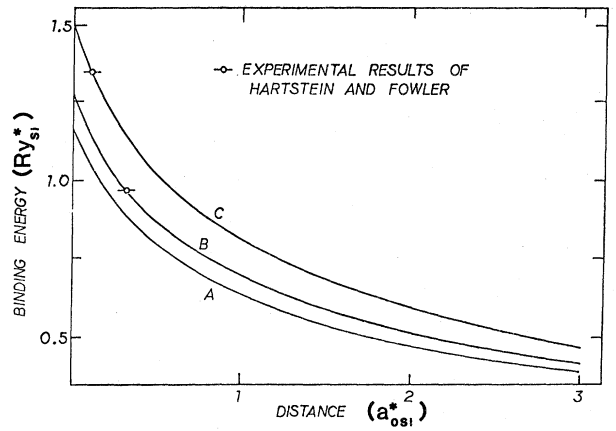

FIG. 9. Binding energy at several field strengths as a function of impurity distance into the silicon dioxide layer. The experimental results of Hartstein and Fowler are also included. Curve A is at 10 esu, curve B is at 19.9 esu and curve C is at 60.4 esu electric field strength.

$$E_b = E(H_0) - E(H) , \tag{2.6}$$

and is dependent upon the electric field through Eqs. (2.2) and (2.3).

This system has been considered by several different authors recently. Martin and Wallis[13] have used a simple variational form to calculate binding energies only when the impurity is located on the interface. Lipari[15] has utilized a basis set which is certainly correct when the impurity is on the interface, but may not be so when the impurity is at a finite distance from the semiconductor/oxide interface. Hipolito and Campos[27] have used the variational form of Martin and Wallis to calculate the effect of electrons in the electric subbands screening the impurity potential and thus changing the binding energy. This screening shall not be considered further in this report.

The binding energy of an electron to a donor impurity located on the interface between the silicon and silicon dioxide as a function of electric field is presented in Fig. 6. The results of Martin and Wallis and those of Lipari, which are the same as in the present calculation are presented. Because of the simple variational form, the results of Martin and Wallis are inferior, giving less binding than those of Lipari and of the present calculation. The binding energy given in Fig. 6 is larger than that found experimentally by Hartstein and Folwer, but as shall be seen, when the impurity is moved off the interface and into the oxide layer the binding energy decreases.

The binding energy of the electron at zero field is exhibited in Figs. 7 and 8 as a function of impurity distance from the interface. In the first of these figures the donor impurity is located in the silicon layer while the second locates the impurity in the silicon dioxide layer. As can be readily seen, there is a large discrepancy between the present calculation and the results of Lipari. This is probably caused by Lipari's use of an inadmissible basis set [in the sense that the trial function employed in a variational solution must obey the same boundary conditions imposed upon the solutions to the Schrödinger equation; see discussion in Paper I (Ref. 16)]. While noting the importance of a boundary condition $\psi=0$ on the interface, Lipari chooses as a basis set

$$\psi_m(\vec{r}) = \sum_i f_i(r) Y_{l_i}^m(\theta,\phi) , \tag{2.7}$$

where

$$f_i(r) = \sum_j C_{ij} e^{-\alpha_j r} , \tag{2.8}$$

and the C_{ij} and α_j are the linear and nonlinear variational parameters, respectively. Later it is noted that only the odd l terms contribute to the ground state in Eq. (2.7) ($m=0$). However, this is only correct when the impurity is located on the interface, and this is illustrated by the coincidence of the results of Lipari and our calculations at $R=0.0$. The point to note in this connection is that the binding energy of the electron decreases more rapidly as a function of impurity distance from the interface (when in the oxide layer) than has been calculated by Lipari.

The electron binding energy to an impurity center located in the oxide layer for several electric field strengths has

TABLE V. Binding energy as a function of impurity distance into the oxide layer for several values of the electric field strength.

R	$\mathscr{E}=0.0$ esu	$\mathscr{E}=10.0$ esu	$\mathscr{E}=19.9$ esu	$\mathscr{E}=60.4$ esu
0.0	0.9423	1.1949	1.2903	1.5062
0.2	0.7327	0.9723	1.0566	1.2373
0.4	0.6143	0.8437	0.9198	1.0762
0.6	0.5347	0.7553	0.8298	0.9627
0.8	0.4763	0.6891	0.7530	0.8762
1.0	0.4311	0.6369	0.6960	0.8070
1.2	0.3949	0.5942	0.6492	0.7499
1.4	0.3650	0.5584	0.6097	0.7017
1.6	0.3398	0.5277	0.5757	0.6602
1.8	0.3183	0.5010	0.5461	0.6239
2.0	0.2996	0.4775	0.5199	0.5920
3.0	0.2336	0.3912	0.4234	0.4747

been calculated and these results are presented in Table V and Fig. 9. Also shown are the experimental results of Hartstein and Fowler, who have found that for electric fields of 19.9 and 60.4 esu, the binding energies are 18 and 25 meV, respectively. These results differ from those of Lipari inasmuch as distance from the interface does not turn out to be the same for both field strengths. The binding energy of 18 meV for the field strength of 19.9 esu occurs for the impurity located at approximately 10 Å, while the 25-meV binding energy at the 60.4-esu field strength occurs for the impurity at ~ 4 Å into the oxide layer. These results demonstrate that agreement with experiment is improved if the impurity ions are located at small, but finite distances from the $Si\text{-}SiO_2$ interface into the insulator. In light of the approximations made in the formulation of the problem, the above results should be regarded as the first step towards a theory in which effects due to screening of the impurity potential, due to electrons in the inversion layer and intervalley coupling, could be quantitatively ascertained.

ACKNOWLEDGMENT

This work was supported by U.S. Department of Energy under Contract No. DE-77-S-05-5489.

[1]See review by T. Ando, A. B. Fowler, and F. Stern, Rev. Mod. Phys. 54, 437 (1982), in particular, Sec. II E.
[2]J. D. Levine, Phys. Rev. 140, 586 (1965).
[3]F. Stern and W. E. Howard, Phys. Rev. 163, 816 (1967).
[4]J. Lauer and T. S. Jayadevarah, Solid State Electron. 16, 644 (1973).
[5]W. Kohn and J. M. Luttinger, Phys. Rev. 98, 915 (1955).
[6]W. Kohn, in *Solid State Physics*, edited by F. Seitz and D. Turnbull (Academic, New York, 1957), Vol. 5, p. 257.
[7]S. T. Pantelides, Rev. Mod. Phys. 50, 797 (1978).
[8]R. J. Bell, W. T. Bousman, Jr., G. M. Goldman, and D. G. Rathbun, Surf. Sci. 7, 293 (1967).
[9]B. V. Petukhov, V. L. Pokrouskii, and V. Chaplik, Fiz. Tverd. Tela (Leningrad) 9, 70 (1967) [Sov. Phys.—Solid State 9, 51 (1967)].
[10]A. A. Karpushin, Fiz. Tverd. Tela (Leningrad) 10, 3515 (1968) [Sov. Phys.—Solid State 10, 2793 (1969)].
[11]A. A. Karpushin, Fiz. Tverd. Tela (Leningrad) 11, 2163 (1969) [Sov. Phys.—Solid State 11, 1748 (1970)].
[12]W. E. Teft, R. Bell and H. V. Romero, Phys. Rev. 177, 1194 (1969); W. E. Teft, and K. R. Armstrong, Surf. Sci. 24, 535 (1971).
[13]B. G. Martin and R. F. Wallis, Phys. Rev. B 18, 5644 (1978).
[14]V. E. Godwin and W. E. Teft, Surf. Sci. 34, 108 (1973).
[15]N. O. Lipari, J. Vac. Sci. Technol. 15, 1412 (1978).
[16]D. B. MacMillen and U. Landman, J. Chem. Phys. 80, 1691 (1984).
[17]A preliminary report of this work has been discussed by D. B. MacMillen and U. Landman, Bull. Am. Phys. Soc. 24, 274 (1979).
[18]L. J. Sham and M. Nakayama, Surf. Sci. 73, 272 (1978).
[19]R. A. Faulkner, Phys. Rev. 184, 713 (1969).
[20]H. L. Davis, J. Chem. Phys. 37, 1508 (1962).
[21]P. O. Löwdin and H. Shull, Phys. Rev. 101, 1730 (1956).
[22]J. O. Hirschfelder and J. F. Kincaid, Phys. Rev. 52, 658 (1937); S. T. Epstein, *The Variational Method in Quantum Chemistry* (Academic, New York, 1974).
[23]B. W. Levinger and D. R. Frankl, J. Phys. Chem. Solids 20, 281 (1961).
[24]J. C. Hensel, H. Hasegawa, and M. Nakayama, Phys. Rev. 138, A225 (1965).
[25]A. Hartstein and A. B. Fowler, Phys. Rev. Lett. 34, 1435 (1975).
[26]A. Hartstein and A. B. Fowler, Surf. Sci. 73, 19 (1978).
[27]O. Hipolite and V. B. Campos, Phys. Rev. B 19, 3083 (1979).